IGF-1 Partially Restores Chemotherapy-Induced Reductions in Neural Cell Proliferation in Adult C57BL/6 Mice

Michelle C. Janelsins[1], **Joseph A. Roscoe**[1], **Michel J. Berg**[2], **Bryan D. Thompson**[3], **Mark J. Gallagher**[2], **Gary R. Morrow**[1,4], **Charles E. Heckler**[1], **Pascal Jean-Pierre**[1], **Lisa A. Opanashuk**[3], and **Robert A. Gross**[2,5]

[1]Department of Radiation Oncology, University of Rochester Medical Center, Rochester, New York, USA

[2]Department of Neurology and Strong Epilepsy Center, University of Rochester Medical Center, Rochester, New York, USA

[3]Department of Environmental Medicine, University of Rochester Medical Center, Rochester, New York, USA

[4]Department of Psychiatry, University of Rochester Medical Center, Rochester, New York, USA

[5]Department of Pharmacology and Physiology, University of Rochester Medical Center, Rochester, New York, USA

Abstract

Chemotherapeutic agents produce persistent difficulties in memory through an unknown mechanism. We tested the hypothesis that chemotherapeutic agents readily able to cross the blood–brain barrier (cyclophosphamide and fluorouracil), as opposed to those not known to readily cross the barrier (paclitaxel and doxorubicin), reduce neural cell proliferation following chemotherapy. We found that 5-bromo-2-deoxyuridine labeling following chemotherapy given to C57BL/6 mice revealed a similar reduction in neural cell proliferation in the dentate gyrus for all four agents. Insulin-like growth factor 1, a molecule implicated in promoting neurogenesis, counteracted the effects of high doses of chemotherapy on neural cell proliferation.

Keywords

Chemotherapy; Cancer treatment; Cognitive impairment; Neural cell proliferation; Neurogenesis; IGF-1

INTRODUCTION

Cancer treatment has markedly increased survivorship over the past three decades, with over 10 million survivors living in the United States today (1,2). Unfortunately, chemotherapy, a mainstay of anticancer therapy, may cause cognitive impairment, frequently termed "chemobrain" (3). While the phenomenon of chemobrain is well documented from a clinical perspective, the etiology of this condition is not understood. Neuropsychological and self-

report assessments during and following chemotherapy reveal deficits including memory lapses, trouble concentrating, difficulty in word association, confusion, trouble multitasking, and slow thinking and information processing (3,4). These problems are most common and most severe during and just after treatment (5) and are more pronounced in those who received high-dose chemotherapy (6). Some patients have chemotherapy-related cognitive problems that last for 5 years or more after treatment (7). These observations suggest that managing the adverse neurobehavioral effects of chemotherapy during the course of treatment and early after treatment could prevent the onset or persistence of cognitive complications in cancer patients and survivors. Findings from a small number of neuroimaging studies showing that chemotherapy affects specific brain areas support this hypothesis. Location-specific brain dysfunction is supported by magnetic resonance imaging (MRI) studies that have identified abnormalities in brain metabolism and blood flow in areas involved in cognition including the prefrontal lobe, hippocampus, parahippocampal gyrus, cingulate gyrus, and precuneus regions (8,9).

Disruption of neurogenesis is one possible mechanism by which chemotherapy may cause cognitive problems. Neurogenesis, a process by which new neurons are generated from newly birthed neural precursors, has been well characterized in the subventricular zone (SVZ) and the subgranular zone (SGZ) of the dentate gyrus (10). Newly birthed cells in the SVZ migrate to the olfactory bulb where they incorporate into the neuronal network, whereas newly birthed cells from the SGZ populate the granule cell network within the dentate gyrus. The dentate gyrus connects to the parahippocampal gyrus including the entorhinal cortex as well as the cornu ammonis (CA) layers of the hippocampus and is primarily involved in memory formation. Fluorouracil, an inhibitor of thymidylate synthase (11) and a commonly used chemotherapy agent that readily crosses the blood–brain barrier (BBB), impairs spatial working memory and also reduces the number of newborn neural precursors and neurons in animal model studies (12,13), thus linking neurogenesis and memory as targets of chemotherapy. Methotrexate, an inhibitor of folic acid synthesis, and thus an inhibitor of purine base synthesis, has also been shown to reduce hippocampal cell proliferation that is linked to spatial learning deficits in rats (14).

Growth factors, hormones, neurotransmitters, and environmental factors influence the survival, proliferation, and differentiation (10,15) of neural progenitor cells. In the SGZ, where neurogenesis is related to memory, relevant growth factors include brain-derived neurotrophic factor (BDNF), vascular endothelial growth factor (VEGF), fibroblast growth factor (FGF), and insulin-like growth factor 1 (IGF-1) (15). Preclinical studies in rats have shown that IGF-1 administration reversed the cognitive decline and reduction in neurogenesis that normally occurs with age, providing evidence that growth factor-promoted neurogenesis is associated with cognition (16,17).

The ability to cross the BBB is characteristic of some common chemotherapeutic agents but not others, and we hypothesized that drugs that easily cross the BBB, compared to those that do not, are more likely to affect neurogenesis. To test that hypothesis, we investigated the effect of four commonly used chemotherapeutic agents on neural cell mitotic activity in the SGZ. Two of the drugs, cyclophosphamide and fluorouracil, readily cross the BBB, and two agents, paclitaxel and doxorubicin, do not. Since IGF-1 promotes neurogenesis, we further explored the possibility that this molecule may protect neural cell proliferation following chemotherapy.

METHODS

Mice

C57BL/6 mice were purchased through Jackson laboratories (Bar Harbor, ME) at 6–8 weeks of age. Upon arrival, all mice were allowed to acclimate to their home cage for 1 week prior to initiation of experiments. All animal housing and procedures were performed in compliance with guidelines established by the University Committee of Animal Resources at the University of Rochester.

Chemotherapeutic paradigms

All chemotherapeutic agents were purchased from Sigma Aldrich (St. Louis, MO). Cyclophosphamide (Cat # C-0768), fluorouracil (Cat # F-6627), paclitaxel (Cat # T-7402), and doxorubicin (Cat # D-1515) were all stored according to manufacturer's instructions until use. All chemotherapeutic agents were diluted in sterile saline. Paclitaxel was sonicated within 2 hr of injection. Groups of C57BL/6 mice were given three intraperitoneal injections of chemotherapeutic agent (cyclophosphamide at 50 mg/kg, fluorouracil at 60 mg/kg, paclitaxel at 5 mg/kg, or doxorubicin at 5 mg/kg), or saline equivalent on days 1, 4, and 7 (n = 6 for each chemotherapy group and n = 8 for the saline control group). On day 8, mice were given a series of 4 intraperitoneal injections of 5-bromo-2-deoxyuridine (BrdU, Cat. # B5002, Sigma Aldrich, St. Louis, MO) at 50 mg/kg which were delivered at 2-hr intervals. Mice were sacrificed 20–24 hr after the first BrdU injection and processed for immunohistochemical analyses.

Weight and physical appearance

We monitored weight in all animals receiving chemotherapy. Mice were weighed prior to their chemotherapy injection and prior to BrdU injection. We also monitored the mice for changes in activity and hair loss although these were not quantified.

IGF-1 experiments

IGF-1 (Cat # GF138) was purchased from Millipore (Billerica, MA). In one cohort, mice were given 40 µg/kg of IGF-1 (or saline) 2 hr prior to three 50 mg/kg doses of cyclophosphamide or saline, and again at 4 and 8 hr after cyclophosphamide or saline administration (n = 6/group). In the second cohort, mice were given 25 µg/kg of IGF (or saline) 2 hr prior to and 4 hr after cyclophosphamide (150 mg/kg) or saline administration (n = 5/group). The following day, a series of 4 BrdU injections was given at 50 mg/kg at 2-hr intervals. Mice were sacrificed 20–24 hr after the first BrdU injection and processed for immunohistochemical analyses.

BrdU immunohistochemistry and cell quantification

All mice were perfused transcardially with 10 mL of sterile saline with heparin followed by 50 mL of 4% paraformaldehyde in 0.1 M phosphate buffer (PB). The brains were isolated, postfixed overnight in 4% paraformaldehyde in 0.1 M PB and transferred to a solution of 30% sucrose in PBS for 5 days prior to coronal sectioning at 50 µm (Figures 2, 3, and 5) or 30 µm (Figure 4) on a freezing Microm HM 400 microtome (Heidelberg, Germany) and storage in cryoprotectant at −20°C prior to immunohistochemical analysis.

Immunohistochemistry was performed on free-floating brain sections. Sections were washed in 6 changes of 0.1 M phosphate buffered saline (PBS) at pH 7.4 for 10 min each to remove cryoprotectant, followed by permeabilization in 0.3% Triton X-100 (Sigma Aldrich, St. Louis, MO) in PBS for 10 min. All incubation steps were done with mild rotation. Tissue sections were then rinsed in 3% hydrogen peroxide (Sigma Aldrich, St. Louis, MO) in PBS

for 30 min to quench endogenous peroxidases. Sections were incubated in 2 N hydrochloric acid (HCl) for 60 min to denature DNA into single strands which allowed the BrdU antibody to bind. Following HCl incubation, tissue sections were rinsed 4 times for 10 min each in 0.3% PBS-Triton X-100. Tissue sections were incubated for 1 hr at room temperature in 10% normal rabbit serum followed by overnight incubation at 4°C in a primary antibody solution containing mouse monoclonal anti-BrdU (1:800, Accurate Chemical, Westbury, NY) in 0.3% PBS-Triton X-100 with 1% normal rabbit serum. Following incubation in the primary antibody solution, sections were washed 3 times for 10 min each at room temperature to remove the unbound primary antibody. Sections were then moved to a secondary antibody solution containing biotinylated rabbit antimouse IgG (1:250, Vector Laboratories, Burlingame, CA) in 0.3% PBS-Triton X-100 and 1% normal rabbit serum for 1 hr at room temperature. Excess secondary antibody was removed with three washes of 0.3% PBS-Triton X-100 for 10 min each. Sections were then incubated in an avidin-biotin-horseradish peroxidase solution (Vector Laboratories, Burlingame, CA) for 1 hr at room temperature. Sections were then washed in 3 rinses of PB for 10 min each and were then incubated in a 3,3′-diaminobenzidine (DAB) fast-tab solution (Sigma Aldrich, St. Louis, MO) for 5 min. Sections were rinsed in PB and mounted onto Superfrost Plus slides (VWR, West Chester, PA), dried, and coverslipped with Clarion mounting media (Electron Microscope Sciences, Hatfield, PA).

Positive cells from sections containing the dentate gyrus were visualized on an Nikon Eclipse 80i microscope (Nikon Instruments, Tokyo, Japan). Brightfield images were captured at 10× magnification with a Spot Camera and Spot Advanced Software Package (Diagnostic Instruments, Sterling Heights, MI). Images were captured from 8 to 15 different tissue sections for each mouse that were taken at every sixth section for those animals cut at 50 µm (Figures 1–3, and 5) and every twelfth section for those animals cut at 30 µm (Figure 4). Positive cells were enumerated for each image using Image Pro software (Media Cybernetics, Silver Spring, MD). A lower threshold of 500 pixels was used for determining a positive cell in these DAB stained sections. The total number of cells per dentate gyrus (GCL, SGZ, and hilus) section was enumerated and sums were calculated for each mouse. We multiplied by the factor necessary to estimate the total number of cells per dentate gyrus based on a 3 mm estimate for the total dentate gyrus volume, a technique commonly used in unbiased stereology for determining the total number of cells in a given structure (18). The estimated sums were averaged for each experimental group. All image capturing and quantification were performed in a blinded fashion.

BrdU and cleaved caspase-3 fluorescent coimmunohistochemistry and colabeled cell quantification

All mice were perfused transcardially and brains were isolated and prepared as described above. Immunohistochemistry was performed on free-floating brain sections. Sections were washed in 6 changes of 0.1M PBS at pH 7.4 for 10 min each to remove cryoprotectant, followed by permeabilization in 0.3% Triton X-100 (Sigma Aldrich, St. Louis, MO) in PBS for 30 min. Tissue sections were incubated in 2 N HCl for 60 min to denature DNA into single strands which made it possible for the BrdU antibody to bind. Following HCl incubation, tissue sections were rinsed 4 times for 10 min each in 0.3% PBS-Triton X-100. Tissue sections were incubated for 1 hr at room temperature in 10% normal goat serum followed by overnight incubation at 4°C in a primary antibody solution containing rat monoclonal anti-BrdU (1:800, Accurate Chemical, Westbury, NY) and rabbit polyclonal anticleaved caspase 3 (1:500, Cell Signaling Technology, Danvers, MA) in 0.3% PBS-Triton X-100 with 1% normal goat serum. Following incubation in the primary antibody solution, sections were washed 3 times for 10 min each at room temperature to remove the unbound primary antibody. Sections were then moved to a secondary antibody solution

containing Alexa Fluor 488 Goat antirat second antibody and Alexa Fluor 568 goat antirabbit (each at 1:250, Molecular Probes, Eugene, OR) in 0.3% PBS-Triton X-100 and 1% normal goat serum for 2 hr, at room temperature. Excess secondary antibody was removed with three washes of 0.3% PBS-Triton X-100 for 10 min each. Sections were rinsed in 3 washes of PB for 15 min each prior to mounting onto Superfrost Plus slides (VWR, West Chester, PA), dried, and coverslipped.

Positive cells from sections containing the dentate gyrus were visualized on an Nikon Eclipse 80i microscope (Nikon Instruments, Tokyo, Japan). Fluorescent images were captured at 20× magnification with a Spot Camera and Spot Advanced Software Package (Diagnostic Instruments, SterlingHeights, MI). Images were captured from 8 to 15 different tissue sections containing the dentate gyrus per mouse, first with a red (568 nm excitation) filter and then with a green (488 nm excitation) filter. The red and green images were then merged in Image Pro software (Media Cybernetics, Silver Spring, MD) to create a third image where the colabeled pixels appeared yellow. Positive cells were then enumerated for each image using Image Pro software as described for enumerating BrdU cells in the DAB protocol above.

Statistical analyses

Data in the tables and figures are expressed as means and their standard errors. Statistical evaluation of the weight data was performed by repeated measures ANOVA with time, treatment, and time by treatment interaction as the fixed effects and an unstructured covariance matrix of the random error component. Hypothesis testing of the fixed effects was performed using F tests with the Kenward–Roger denominator degrees of freedom method (19). For the rest of the analyses, one-way ANOVA using the Dunnett's test for *posthoc* comparisons of group means with control, two-way ANOVA including interaction, or Student's *t* -test were used as indicated. One animal from the control group of Figure 4 was not included in the analysis due to poor BrdU labeling that was not consistent with that of any of the other control animals in any other experiments herein. Otherwise, all data collected was used in the analyses. SPSS Software (Chicago, IL) was used for one-way ANOVA, two-way ANOVA, and Student's *t* -test analyses. SAS v9.2 (Cary, NC) was used for repeated measures ANOVA analyses. In all cases, a *p* value of <.05 was considered statistically significant.

RESULTS

Chemotherapy causes weight loss

We compared weights of mice receiving chemotherapy over days 1, 4, 7, and 8 in control-, fluorouracil-, cyclophosphamide-, paclitaxel-, and doxorubicin-treated animals (Figures 1(a) and (b)). Repeated measures ANOVA revealed significant differences in drug by day interaction ($p < .05$) with effects of fluorouracil and doxorubicin showing the greatest changes in weights at days 7 and 8 compared to control.

For IGF-1 experimental cohorts, there was no significant difference in the weights of any mice in drug by day effects (Figure 4(b)). Mice receiving the single high-dose cyclophosphamide (Figure 5(b)) also experienced significant weight loss from day 1 to day 2 as revealed by a significant drug by treatment effect ($p < .05$).

We observed mice twice daily to determine other physical characteristics of mice receiving chemotherapy and control treatments in all experiments. None experienced hair loss or had apparent decrease in overall activity regardless of treatment group. None died following chemotherapy.

Neural cell division is reduced following administration of chemotherapeutic agents readily able to cross the BBB and those not readily able to cross the BBB in the neurogenic dentate gyrus

We hypothesized that one possible mechanism of chemotherapeutic agent-mediated brain toxicity is the capacity of the drug (i.e., fluorouracil or cyclophosphamide) to readily cross the BBB and directly cause CNS injury. To test this hypothesis, we compared the effects on neural cell proliferation within the SGZ of the dentate gyrus, the site of hippocampal neurogenesis, of commonly used BBB-crossing chemotherapeutic agents (fluorouracil and cyclophosphamide) to those not known to readily cross the BBB (doxorubicin and paclitaxel). We administered chemotherapeutic agents in a multiple-dose regimen (Figure 1(a)) and then identified newly divided cells. We observed a qualitative reduction of BrdU positive cells within the dentate gyrus following administration of all four chemotherapeutic drugs (Figures 2(b)–(e)) in comparison to saline control (Figure 2(a)). A majority of BrdU positive cells enumerated were in the SGZ. Few positive cells were observed in the granule cell layer (GCL) and the hilus and these two regions were also included in the quantitative analyses. Quantitative analyses revealed a 15.4% reduction in BrdU positive cells following fluorouracil and a 30.5% reduction following cyclophosphamide. Similarly, non-BBB crossing agents doxorubicin and paclitaxel led to a 22.4 and a 36.0% reduction in newly divided cells, respectively (mean number of positive cells per dentate gyrus = 2,103.2 in saline-treated animals, 1,776.8 in fluorouracil-treated animals, 1,462.0 in cyclophosphamide-treated animals, 1,632.2 in paclitaxel-treated animals, and 1,360.2 in doxorubicin-treated animals, Figure 2(f), $p < .05$ for all four chemotherapeutic drugs in comparison to saline using one-way ANOVA with Dunnett's test). Furthermore, there was no difference in the extent of cell mitotic activity following delivery of agents readily able to cross the BBB (fluorouracil and cyclophosphamide) compared to those not able to do so (paclitaxel and doxorubicin) ($p > .05$, Student's t-test). In a second study, a single high dose of cyclophosphamide resulted in a 40.9% reduction in newly divided cells in the dentate gyrus (mean number of positive cells per dentate gyrus = 2,336.2 in the saline group compared to 1,381.4 in the cyclophosphamide treated animals, Figures 5(c), (e), and (g), $p < .05$ using a two-tailed Student's t-test) as compared to the 30.5% reduction seen in the multiple-dose regimen.

Chemotherapy causes a decrease in proliferation rather than apoptosis in newly divided cells in the neurogenic dentate gyrus

In order to determine if the reduction in newly divided cells following chemotherapy was caused by an increase in apoptosis, we performed coimmunohistochemistry for BrdU and cleaved caspase-3 in all chemotherapy-treated mice. Quantitative analyses revealed no significant difference in the number of BrdU and caspase-3 double positive cells following chemotherapy in any treatment group from the multiple-dose paradigm Figures 3(a)–(e) and (g), $p > .05$ in one-way ANOVA with Dunnett's test) or in the single high-dose cyclophosphamide group compared to control (Figures 3(a), (f), and (h), $p > .05$ using a two-tailed Student's t-test), further supporting our hypothesis that chemotherapy reduces neural cell proliferation in the SGZ of the dentate gyrus.

IGF-1 improves neural cell proliferation that is reduced in the presence of high-dose cyclophosphamide chemotherapy

Cyclophosphamide is a mainstay of adjuvant chemotherapy for breast cancer and "chemobrain" is frequent in those receiving cyclophosphamide-based treatments. Because IGF-1 can promote neurogenesis within the CNS (20), it is a potential therapeutic agent for improving reduced SGZ cell proliferation resulting from cyclophosphamide chemotherapy. We administered IGF-1 subcutaneously prior to and following a conventional multiple-dose cyclophosphamide chemotherapy regimen (Figure 4(a)) and a single high-dose

cyclophosphamide chemotherapy regimen (Figure 5(a)) to assess its effects on neural cell proliferation. IGF-1 did not significantly increase the number of newly divided neural precursors after multiple doses of cyclophosphamide chemotherapy (mean number of positive cells in the dentate gyrus = 3,375.8 in the IGF-1/cyclophosphamide treated group compared to 3,174.0 in the saline/cylcophosphamide group (Figure 4(g), $p > .05$ using a two-way ANOVA test for the drug by IGF-1 interaction). However, as in the previous experiment, cyclophosphamide did produce a significant 23% reduction in newly divided cells (Figures 4(c), (e), and (g), $p < .05$ using a two-way ANOVA test for drug effect).

In the high-dose cyclophosphamide chemotherapy model, IGF-1 increased the number of new cells in the dentate gyrus, compared to those mice given saline, by 27.5% (mean number of cells per dentate gyrus = 1,660.8 in the IGF-1/cyclophosphomide group compared to 1,381.4 in the saline/cyclophosphamide group, Figures 5(c)–(g), $p < .05$ in two-way ANOVA drug by IGF-1 interaction).

DISCUSSION

An understanding of the mechanisms of chemotherapy-related cognitive dysfunction may inform the creation of interventions to alleviate these symptoms (4), a process that would be aided by the development of a preclinical model of chemotherapy-related cognitive decline. Our results show, contrary to our expectations, that chemotherapeutic agents reduce the number of newly divided cells within the SGZ of the dentate gyrus, whether or not the agents are known to cross the blood–brain barrier. This result was surprising given that the chemotherapeutic agents paclitaxel and doxorubicin are very susceptible to BBB resistance by p-glycoprotein efflux mechanisms (21). Because chemotherapeutic agents target cancer cells at least partly by modifying DNA and impeding cell division, a possible explanation of these findings may be that although paclitaxel and doxorubicin are not thought to readily cross the BBB, they may be able to penetrate at levels sufficient to affect rapidly dividing cells in neurogenic regions of the brain and cause sustained neurotoxicity. Future studies should assess levels of chemotherapeutic agent levels in the brain following chemotherapy at this time point to see if a correlation between drug levels and reduced neural cell proliferation in the dentate gyrus exists.

We observed that subcutaneous delivery of IGF-1 in our chemotherapy paradigms led to an increased number of newly formed cells in the dentate gyrus in mice that received high-dose cyclophosphamide chemotherapy compared to mice that received subcutaneous delivery of the saline control and chemotherapy. In the multiple-dose paradigm, the number of BrdU positive cells was higher in the IGF-1/Cyclophosphamide group compared to similarly injected mice with saline and cyclophosphamide, although this result was not significant. This could be due to a lack of a sustained protective effect of IGF-1 over multiple doses of chemotherapy or to insensitivity in our methods to detect such a difference in that cohort of mice.

Our data support the literature showing that IGF-1 promotes proliferation of neural progenitors within the same time-frame in which we have investigated newly divided neural cells in our high-dose chemotherapy paradigm (20,22,23). The observation that IGF-1 resulted in only a partial rescue of the number of newly divided neural cells may be the consequence of the requirement for many growth factors and neurotransmitters to regulate the neurogenic process within the SGZ microenvironment (10). It is still unclear how chemotherapy affects levels of circulating IGF-1, other growth factors, and neurotransmitters that are also important for proper neurogenesis to occur. Since the promoted proliferation of neural progenitors by IGF-1 is linked to improved memory

observed in other animal studies (17), IGF-1 may also improve cognitive impairment in our chemotherapy model, a focus of future studies.

To what extent our results are generalizable to a human population is uncertain, if only because human treatment regimens often consist of multiple agents administered in multiple treatment phases. Nevertheless, our data suggest that both chemotherapeutic agents that are known to readily cross the BBB and those that are not thought to readily cross the BBB have similar negative effects on cell proliferation within the dentate gyrus. Future studies will investigate the long-term effects of chemotherapeutic agents on cell proliferation in the dentate gyrus, specific cell types affected at acute time points and longer time points, and specific mechanisms involving IGF-1 and its action in reversing diminished neural cell proliferation seen following chemotherapy.

Reduced neurogenesis following chemotherapy may have broader implications. Neurogenesis can also be altered by stress, anxiety, sleep disorders, and depression (10,24–26); all are common symptoms experienced by cancer patients (4). For example, stress-induced studies in mice revealed that heightened glucocorticoid levels caused by activation of the hypothalamic-pituitary-adrenal axis are a major cause of decreases in SGZ cell proliferation. Thorough studies in animal models are needed to understand the effects of chemotherapy on neurogenesis and memory, and the effects involving other symptoms; our studies, along with others in the field, suggest a first step and a reasonable model. Ultimately, we wish to understand to what extent reduced neurogenesis may occur in patients and how to limit its deleterious effects.

Acknowledgments

REFERENCES

1. American Cancer Society. Cancer Facts and Figures 2008. Atlanta, GA: American Cancer Society; 2008.

2. Ganz PA. A teachable moment for oncologists: cancer survivors, 10 million strong and growing! J Clin Oncol. 2005; 23(24):5458–5460. [PubMed: 16043826]

3. Vardy J, Rourke S, Tannock IF. Evaluation of cognitive function associated with chemotherapy: a review of published studies and recommendations for future research. J Clin Oncol. 2007; 25(17): 2455–2463. [PubMed: 17485710]

4. Bower JE. Behavioral symptoms in patients with breast cancer and survivors. J Clin Oncol. 2008; 26(5):768–777. [PubMed: 18258985]

5. Wefel JS, Lenzi R, Theriault RL, Davis RN, Meyers CA. The cognitive sequelae of standard-dose adjuvant chemotherapy in women with breast carcinoma: results of a prospective, randomized, longitudinal trial. Cancer. 2004; 100(11):2292–2299. [PubMed: 15160331]

6. van Dam FS, Schagen SB, Muller MJ, Boogerd W, vd Wall E, Droogleever Fortuyn ME, Rodenhuis S. Impairment of cognitive function in women receiving adjuvant treatment for high-risk breast cancer: high-dose versus standard-dose chemotherapy. J Natl Cancer Inst. 1998; 90(3):210–218. [PubMed: 9462678]

7. Schultz PN, Beck ML, Stava C, Vassilopoulou-Sellin R. Health profiles in 5836 long-term cancer survivors. Int J Cancer. 2003; 104(4):488–495. [PubMed: 12584748]

8. Inagaki M, Yoshikawa E, Matsuoka Y, Sugawara Y, Nakano T, Akechi T, Wada N, Imoto S, Murakami K, Uchitomi Y. Smaller regional volumes of brain gray and white matter demonstrated in breast cancer survivors exposed to adjuvant chemotherapy. Cancer. 2007; 109(1):146–156. [PubMed: 17131349]

9. Saykin AJ, Ahles TA, McDonald BC. Mechanisms of chemotherapy-induced cognitive disorders: neuropsychological, pathophysiological, and neuroimaging perspectives. Semin Clin Neuropsychiatry. 2003; 8(4):201–216. [PubMed: 14613048]

10. Zhao C, Deng W, Gage FH. Mechanisms and functional implications of adult neurogenesis. Cell. 2008; 132(4):645–660. [PubMed: 18295581]

11. Parker WB, Cheng YC. Metabolism and mechanism of action of 5-fluorouracil. Pharmacol Ther. 1990; 48(3):381–395. [PubMed: 1707544]

12. Mustafa S, Walker A, Bennett G, Wigmore PM. 5-Fluorouracil chemotherapy affects spatial working memory and newborn neurons in the adult rat hippocampus. Eur J Neurosci. 2008; 28(2): 323–330. [PubMed: 18702703]

13. Dietrich J, Han R, Yang Y, Mayer-Proschel M, Noble M. CNS progenitor cells and oligodendrocytes are targets of chemotherapeutic agents in vitro and in vivo. J Biol. 2006; 5(7):22. [PubMed: 17125495]

14. Seigers R, Schagen SB, Beerling W, Boogerd W, van Tellingen O, van Dam FS, Koolhaas JM, Buwalda B. Long-lasting suppression of hippocampal cell proliferation and impaired cognitive performance by methotrexate in the rat. Behav Brain Res. 2008; 186(2):168–175. [PubMed: 17854921]

15. Lledo PM, Alonso M, Grubb MS. Adult neurogenesis and functional plasticity in neuronal circuits. Nat Rev Neurosci. 2006; 7(3):179–193. [PubMed: 16495940]

16. Lichtenwalner RJ, Forbes ME, Bennett SA, Lynch CD, Sonntag WE, Riddle DR. Intracerebroventricular infusion of insulin-like growth factor-I ameliorates the age-related decline in hippocampal neurogenesis. Neuroscience. 2001; 107(4):603–613. [PubMed: 11720784]

17. Markowska AL, Mooney M, Sonntag WE. Insulin-like growth factor-1 ameliorates age-related behavioral deficits. Neuroscience. 1998; 87(3):559–569. [PubMed: 9758223]

18. West MJ, Slomianka L, Gundersen HJ. Unbiased stereological estimation of the total number of neurons in the subdivisions of the rat hippocampus using the optical fractionator. Anat Rec. 1991; 231(4):482–497. [PubMed: 1793176]

19. Kenward MG, Roger JH. Small sample inference for fixed effects from restricted maximum likelihood. Biometrics. 1997; 53(3):983–997. [PubMed: 9333350]

20. Anderson MF, Aberg MA, Nilsson M, Eriksson PS. Insulin-like growth factor-I and neurogenesis in the adult mammalian brain. Brain Res Dev Brain Res. 2002; 134(1–2):115–122.

21. Schinkel AH. P-Glycoprotein, a gatekeeper in the blood-brain barrier. Adv Drug Deliv Rev. 1999; 36(2–3):179–194. [PubMed: 10837715]

22. Aberg MA, Aberg ND, Hedbacker H, Oscarsson J, Eriksson PS. Peripheral infusion of IGF-I selectively induces neurogenesis in the adult rat hippocampus. J Neurosci. 2000; 20(8):2896–2903. [PubMed: 10751442]

23. Aberg MA, Aberg ND, Palmer TD, Alborn AM, Carlsson-Skwirut C, Bang P, Rosengren LE, Olsson T, Gage FH, Eriksson PS. IGF-I has a direct proliferative effect in adult hippocampal progenitor cells. Mol Cell Neurosci. 2003; 24(1):23–40. [PubMed: 14550766]

24. Mirescu C, Gould E. Stress and adult neurogenesis. Hippocampus. 2006; 16(3):233–238. [PubMed: 16411244]

25. Santarelli L, Saxe M, Gross C, Surget A, Battaglia F, Dulawa S, Weisstaub N, Lee J, Duman R, Arancio O, Belzung C, Hen R. Requirement of hippocampal neurogenesis for the behavioral effects of antidepressants. Science. 2003; 301(5634):805–809. [PubMed: 12907793]

26. Mirescu C, Peters JD, Noiman L, Gould E. Sleep deprivation inhibits adult neurogenesis in the hippocampus by elevating glucocorticoids. Proc Natl Acad Sci U S A. 2006; 103(50):19170–19175. [PubMed: 17135354]
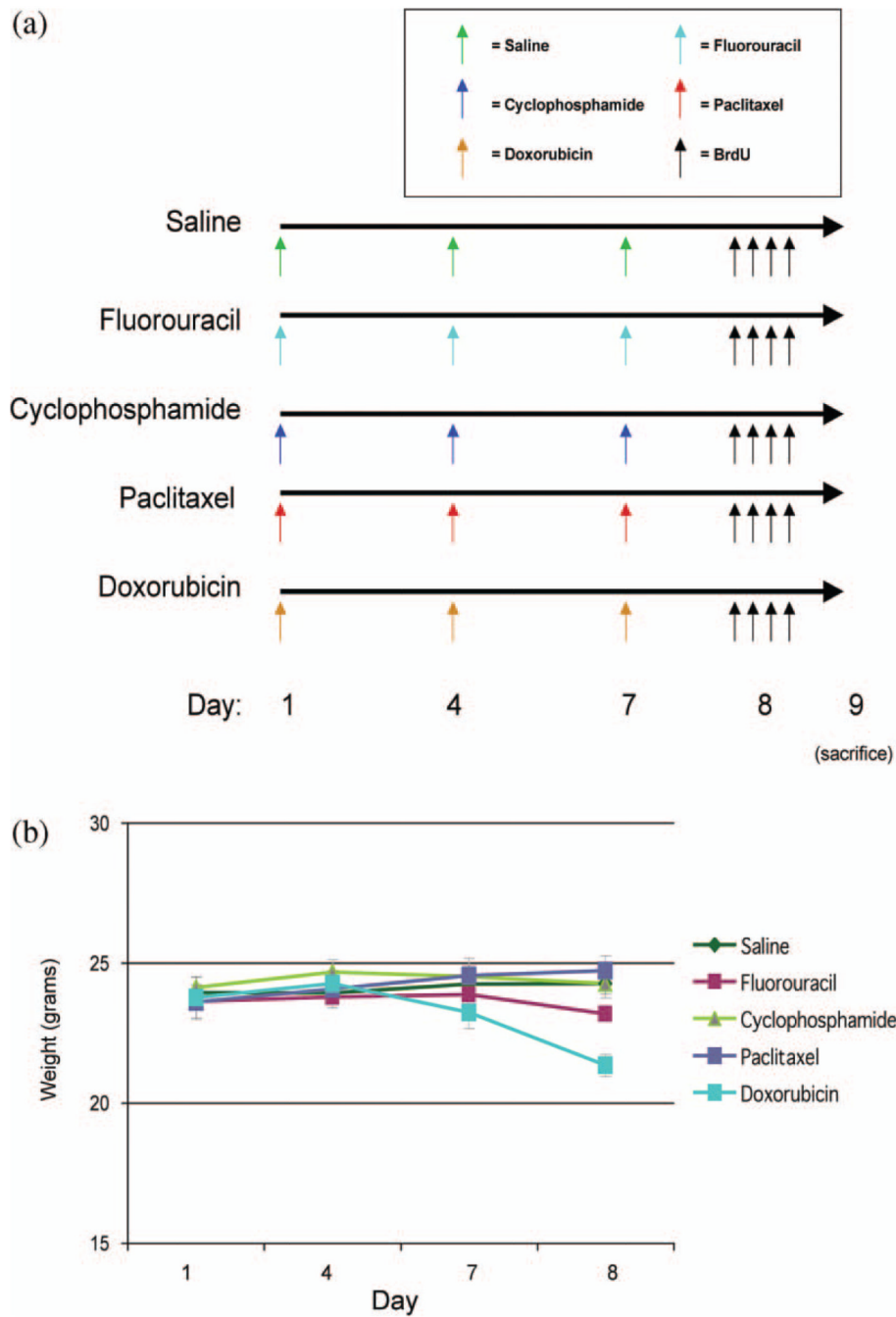
Figure 1.
Paradigms used to investigate differences in neural cell proliferation in the neurogenic dentate gyrus following administration of chemotherapeutic agents readily able to cross the BBB and those agents not readily able to cross the BBB. (a) Six–eight week old C57BL/6 mice were injected intraperitoneally with saline (control), fluorouracil, cyclophosphamide, placlitaxel, or doxorubicin on days 1, 4, and 7 ($n = 6$–8/group). On day 8, mice were injected intraperitoneally 4 times with BrdU to label newly divided cells. On day 9, (20–24 hr after the first BrdU injection), mice were sacrificed by transcardiac perfusion, and brains were isolated and processed for immunohistochemical analysis. (b) Mouse weights were recorded each morning prior to chemotherapy (day 1, 4, and 7) and the morning after chemotherapy

(day 8). Significant differences were determined by repeated measures ANOVA considering a $p < .05$ for drug by day effects to be considered statistically significant.
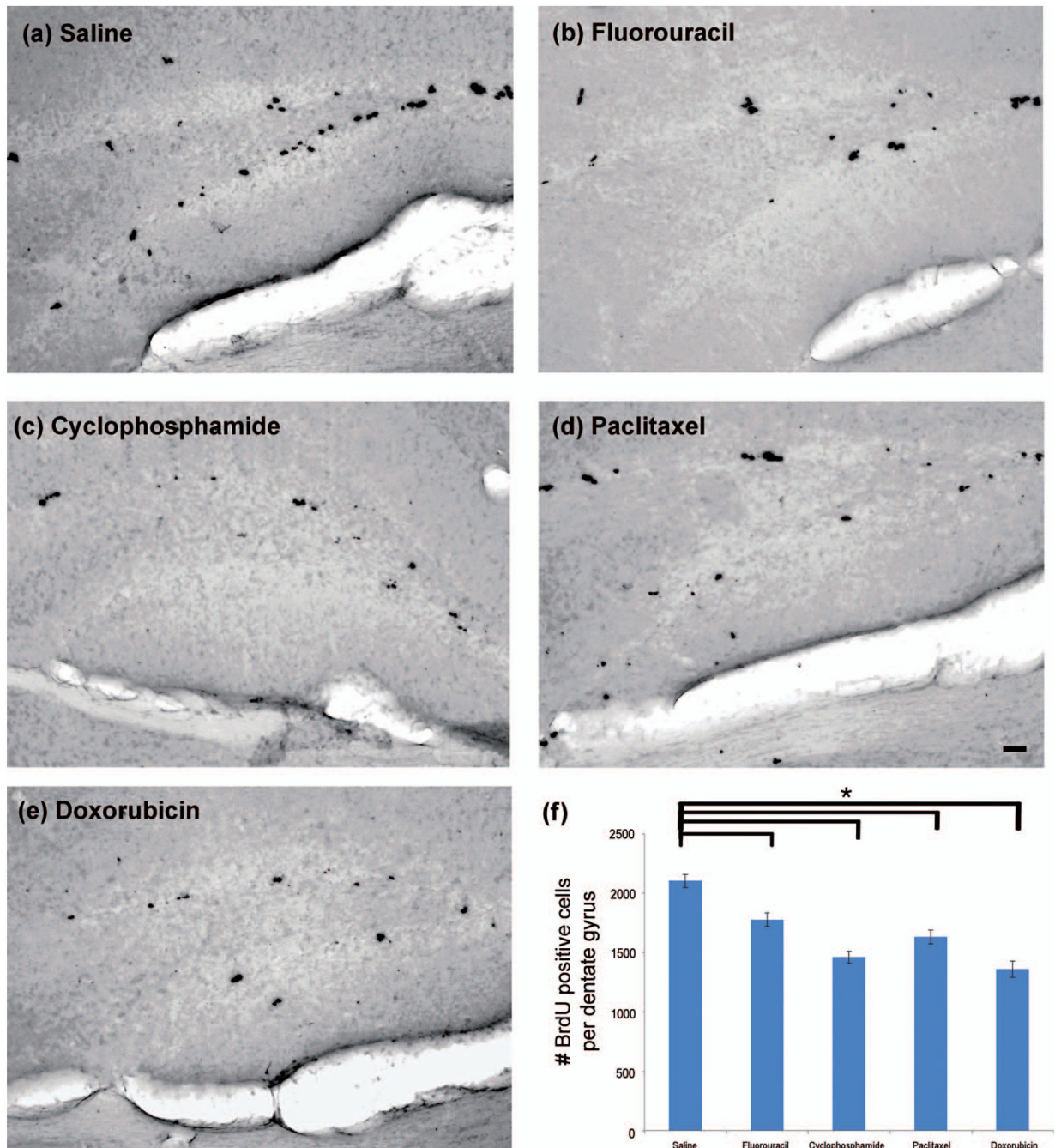
Figure 2.
Chemotherapeutic agents readily able to cross the BBB and those not readily able to cross the BBB result in a similar reduction in the number of newly divided neural cells in the neurogenic dentate gyrus. Brains were sectioned coronally at 50 µm, and immunohistochemistry was performed on every sixth section of the dentate gyrus for a total of approximately 8 free-floating sections per animal ($n = 6$–8/group) using the DAB method. (a–e) Representative photomicrographs display BrdU positive cells mostly within the SGZ of the dentate gyrus for each experimental group. Images of the dentate gyrus were captured, and positive cells within the SGZ, GCL and hilus were enumerated for each mouse. (f) Data are expressed as the averaged number of BrdU positive cells per dentate gyrus for each

group. One-way ANOVA was performed with Dunnett's test using saline as the control. The "*" indicates a significant ($p < .05$) difference compared with the saline control. The scale bar represents 50 µm.
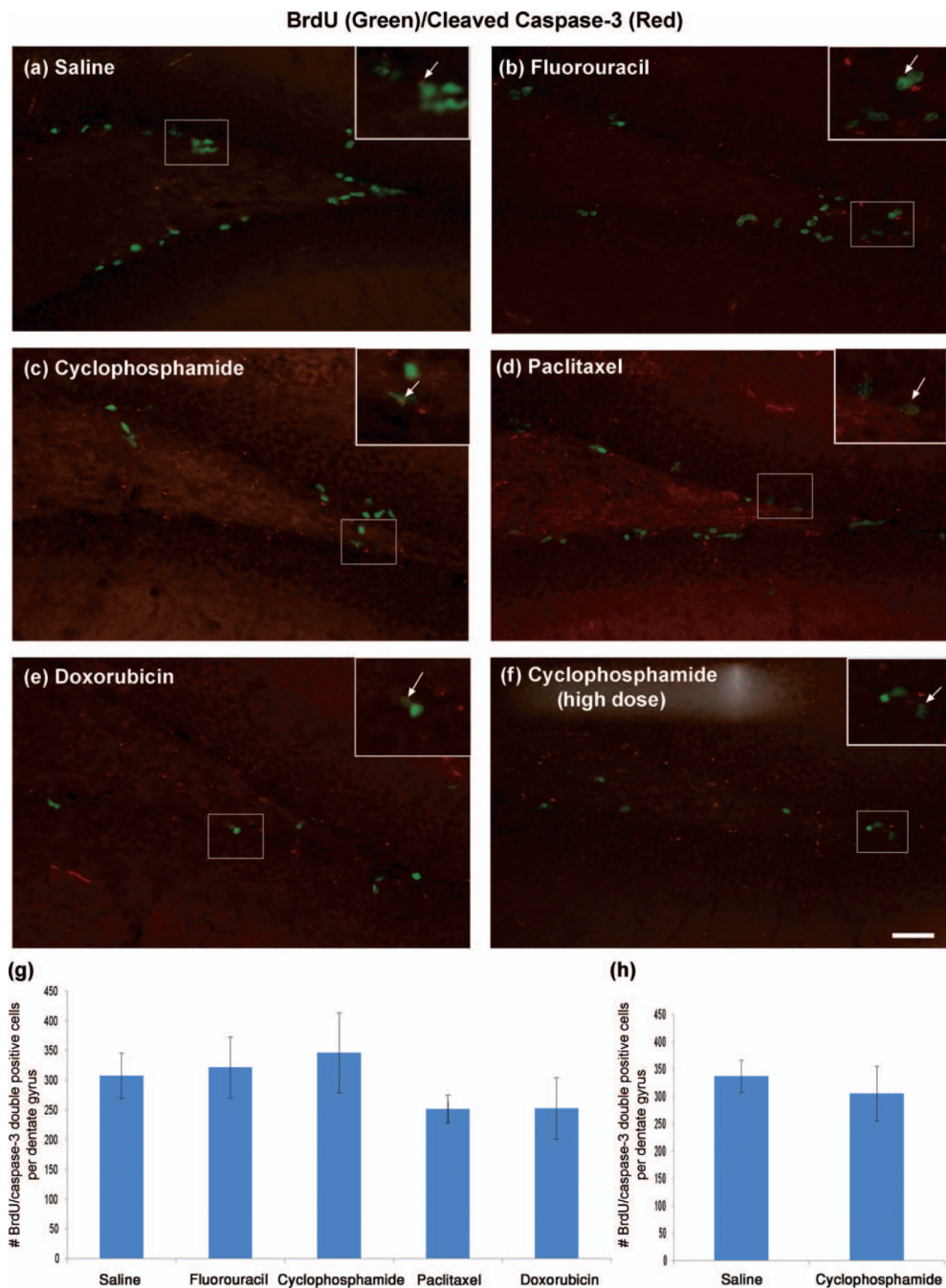
Figure 3.
Chemotherapy causes a decrease in proliferation rather than apoptosis in newly divided cells in the neurogenic dentate gyrus. Brains were sectioned coronally at 50 µm, and coimmunohistochemistry was performed on every sixth section of the dentate gyrus for a total of approximately 8 free-floating sections per animal ($n = 6$–8/group) using fluorescence to identify colabeled BrdU and cleaved caspase-3 cells in the dentate gyrus. (a–f) Representative photomicrographs show the merged image of BrdU (green) and cleaved caspase-3 (red) coimmunohistochemistry. Inserts represent digitally enhanced areas of the image to specify colabeled staining. (g and h) Data are expressed as the averaged number of BrdU and caspase-3 double positive cells per dentate gyrus for each group. One-way

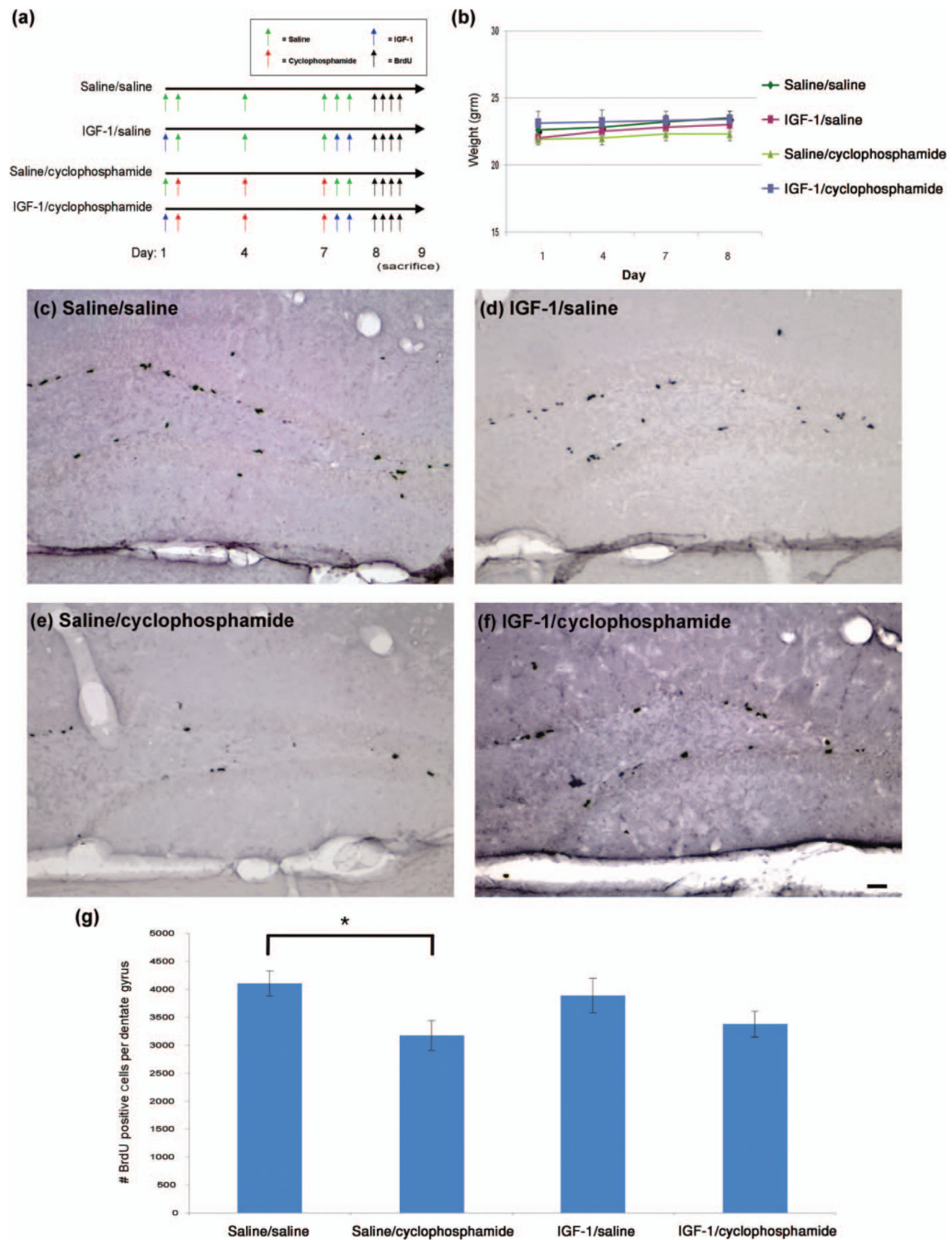ANOVA was performed with Dunnett's test with saline as the control. The scale bar represents 50 μm.

Figure 4.
IGF-1 does not significantly increase the number of newly divided neural cells in the neurogenic dentate gyrus following a multiple-dose cyclophosphamide chemotherapy regimen. (a) Two hours prior to chemotherapy, mice were subcutaneously injected with saline control or IGF-1. Cyclophosphamide chemotherapy was administered intraperitoneally on days 1, 4, and 7 ($n = 6$/group). Four hours following chemotherapy on day 7, mice were given 2 injections of IGF-1 that were given 4 hr apart. On day 8, mice were injected intraperitoneally 4 times with BrdU to label newly divided cells. On day 9 (20–24 hr after the first BrdU injection), mice were sacrificed by transcardiac perfusion, and brains were isolated and processed for immunohistochemistry. (b)Weights were obtained the

morning just prior to chemotherapy on days 1, 4, and 7 and the morning after chemotherapy (day 8). Significant differences were determined by repeated measures ANOVA considering a $p < .05$ for drug by day effects to be considered statistically significant. (c–f) Brains were sectioned coronally at 30 µm, and BrdU immunohistochemistry was performed on every twelfth section for a total of approximately 15 free-floating sections per animal for immunohistochemistry. DAB immunohistochemistry, image capturing and cell quantification were all performed as in Figure 2. (g) Two-way ANOVA was performed with tests for drug effect and cyclophosphamide by IGF-1 interaction. The "*" indicates a significant ($p < .05$) difference. The scale bar represents 50 µm.
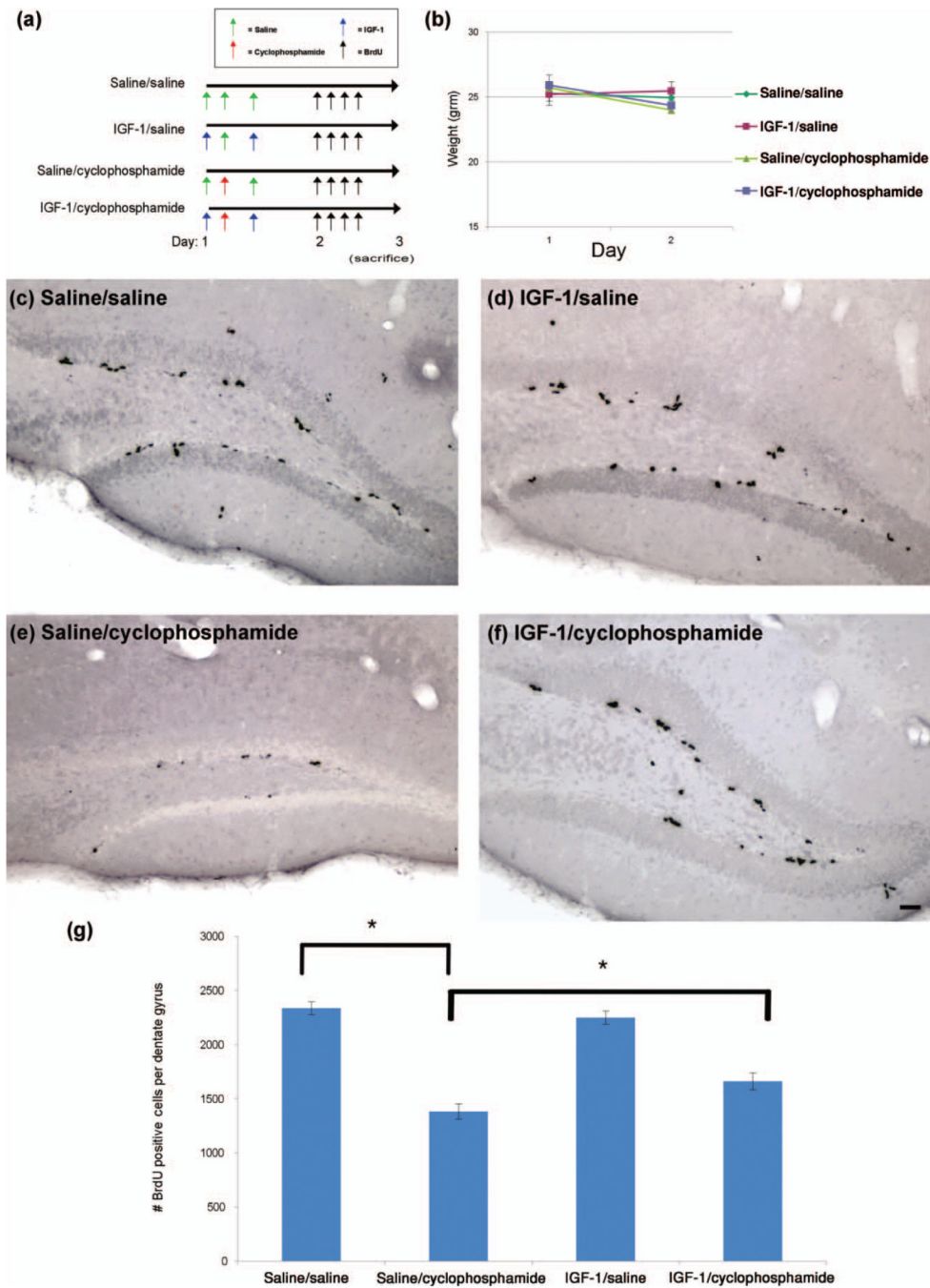
Figure 5.
IGF-1 significantly increases the number of newly divided neural cells in the neurogenic dentate gyrus following a single high-dose chemotherapy regimen. (a) Two hours prior to chemotherapy, mice were subcutaneously injected with saline control or IGF-1. Cyclophosphamide chemotherapy was administered intraperitoneally. Four hours following chemotherapy, mice were given another saline or IGF-1 injection ($n = 5$/group). The next day, mice were injected intraperitoneally 4 times with BrdU to label newly divided cells. On the third day (20–24 hr after the first BrdU injection), mice were sacrificed by transcardiac perfusion, and brains were isolated and processed for immunohistochemistry. (b) Weights were obtained the morning just prior to chemotherapy on days 1, and the morning after

chemotherapy (day 2). Significant differences were determined by repeated measures ANOVA considering a $p < .05$ for drug by day effects to be considered statistically significant. (c–f) Brains were sectioned coronally at 50 µm, and DAB immunohistochemistry, image capturing, and cell quantification were all performed as in Figure 4. (g) Two-way ANOVA was performed with tests for drug effect and cyclophosphamide by IGF-1 interaction. The "*" indicates a significant ($p < .05$) difference. The scale bar represents 50 µm.